Mon. Not. R. Astron. Soc. **357,** 961–966 (2005) doi:10.1111/j.1365-2966.2005.08693.x

The chemistry of transient microstructure in the diffuse interstellar medium

T. A. Bell,[1⋆] S. Viti,[1] D. A. Williams,[1] I. A. Crawford[2] and R. J. Price[1]

[1]*Department of Physics & Astronomy, University College London, Gower Street, London WC1E 6BT*
[2]*School of Earth Sciences, Birkbeck College, Malet Street, London WC1E 7HX*

Accepted 2004 December 1. Received 2004 October 5; in original form 2004 April 16

ABSTRACT

Transient microstructure in the diffuse interstellar medium (ISM) has been observed towards Galactic and extragalactic sources for decades, usually in lines of atoms and ions, and, more recently, in molecular lines. Evidently, there is a molecular component to the transient microstructure. In this paper, we explore the chemistry that may arise in such microstructure. We use a photodissociation region (PDR) code to model the conditions of relatively high density, low temperature, very low visual extinction and very short elapsed time that are appropriate for these objects. We find that there is a well-defined region of parameter space where detectable abundances of molecular species might be found. The best matching models are those where the interstellar microstructure is young ($<$100 yr), small ($\sim$100 au) and dense ($>10^4$ cm^{-3}).

Key words: ISM: molecules – ISM: structure.

1 INTRODUCTION

Observational evidence for microstructure on a Solar system scale in the diffuse interstellar medium (ISM) has been accumulating for the last three decades. Measurements include very long baseline interferometry (VLBI) of H atom 21 cm absorption towards extragalactic sources (Dieter, Welch & Romney 1976; Diamond et al. 1989; Davis, Diamond & Goss 1996), absorption of atomic lines towards transversely moving pulsars (Frail et al. 1994), absorption differences towards stellar binaries (Meyer & Blades 1996; Lauroesch, Meyer & Blades 2000) and towards multiple systems and clusters (Kemp, Bates & Lyons 1993; Langer, Prosser & Sneden 1990; Lauroesch & Meyer 1999), and secular variations over intervals of a few years along the line of sight to single stars (Hobbs et al. 1991; Danks & Sembach 1995; Blades et al. 1997; Cha & Sembach 2000; Crawford et al. 2000; Price, Crawford & Barlow 2000; Danks et al. 2001; Welty & Fitzpatrick 2001). Marscher, Moore & Bania (1993) find secular changes in formaldehyde absorption towards extragalactic sources, the first report of molecular tracers of microstructure. Moore & Marscher (1995) infer structure on scales of order 10 au, with number densities possibly larger than 10^6 cm^{-3}, from further formaldehyde observations towards extragalactic sources. They also find spatial variations in formaldehyde and hydroxyl absorption line profiles towards the extended radio galaxy 3C 111. Lucas & Liszt (1993) and Liszt & Lucas (2000) have used similar observations to explore the range of chemistry in diffuse and translucent clouds. It is also well known (Falgarone, Puget & Perault 1992) that structure at larger scales ($\sim$ 0.01 pc) exists in nearby clouds.

Crawford (2002) has recently detected absorption in lines of CH at the specific velocity (different to that of the surrounding medium) of a previously reported variable component in the line of sight to κ Vel. Using a simple chemical model, Crawford obtained a value for the number density of the CH-containing microstructure towards κ Vel that was consistent with the density inferred from measurements of the Ca I/Ca II ratio at the same velocity component: $n_{\rm H} \sim 10^3$ cm^{-3}. The measured CH column density would require the path-length to be more than 1 order of magnitude larger than the assumed transverse size, supporting the view that the structure may be extended in the line of sight, either as a filament or a sheet.

The most detailed study of molecular microstructure to date has been made by Rollinde et al. (2003). These authors made spectroscopic observations of the runaway reddened star HD 34078 (whose velocity transverse to the line of sight is $\sim$100 km s^{-1}) over a 3-yr period, supplemented by data from earlier epochs, to probe the foreground cloud distributions of CH, CH$^+$, CN and DIB carriers on scales from 1–150 au. Their results show that the CH column density increased by 20 per cent in 10 yr while the CH$^+$ column density and two DIB strengths were unchanged. The CN column density shows a modest rise in this period.

Although some authors have argued that some of the radio evidence for microstructure is flawed by poor data handling (e.g. Stanimirovic et al. 2003), the evidence in favour of the existence of microstructure now seems overwhelming. The general conclusion is that microstructure has a scale of 10–100 au and has typical densities much larger than the ambient interstellar density. The transverse visual extinction is therefore very small and the gas in the structure can only be poorly shielded from the interstellar radiation field.

⋆E-mail: tab@star.ucl.ac.uk

© 2004 RAS

The origin of the microstructure has been the subject of intense study (Pety & Falgarone 2000; Gwinn 2001). Some authors argue that it cannot originate through non-magnetic hydrodynamics and it has been suggested that it may be excited in regions of high magnetic pressure by slow-mode magnetosonic waves (Hartquist, Falle & Williams 2003). However it is formed, it is overpressured and must be transient. Rollinde et al. (2003) inferred from their observations that the variations were not the result of dense clumps passing through the line of sight. We are inclined to agree with their conclusion on dynamical grounds and emphasize that the transience of the microstructure implied by the high overpressure must affect the chemistry. It is unclear whether these structures are extended, i.e. filamentary or sheet-like, or whether they are compact objects. Extended objects could have longer path-lengths along the line of sight, if the orientation is suitable, and therefore the constraints on density could be relaxed as compared with compact objects. The geometry may be related to the origin of these objects.

The purpose of this paper is to explore the chemistry that may arise in the conditions apparently appropriate for the transient microstructure: rapid transition from relatively low to relatively high density, low temperature, very low transverse visual extinction, and subject to the normal interstellar radiation and particle fields. In Section 2, we describe the model in more detail, and present in Section 3 our predictions of detectable chemistry as functions of time and depth into the slab. In Section 4, we describe the region of parameter space in which detectable molecular column densities might be found and discuss the relevance of possible detections to the geometry of the structure.

2 THE MODEL

We model the region crudely as a semi-infinite slab illuminated from one side; the density rises as a step function at the edge of the slab. We compute the chemistry as a function of time and transverse depth position within the slab, restricting our attention to the edge region (see Fig. 1). What is unusual about this calculation compared with other studies of diffuse clouds is that the region of interest into the slab transversely to the line of sight is restricted to $\sim$10 au and to a very short evolutionary age, typically less than 10^3 yr. These tiny spatial and time domains are usually ignored in studies of diffuse clouds (but note the models proposed by Cecchi-Pestellini & Dalgarno 2000 to account for H_3^+ and other species in the line of sight towards Cygnus OB2). We have therefore had to develop a chemical code in which particular attention is given to early time and edge effects. This code is a development of the photodissociation region (PDR) code written by Viti and Thi (Papadopoulos, Thi & Viti 2002).

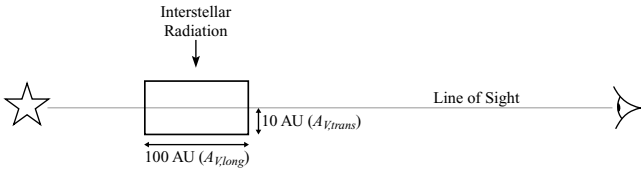

Figure 1. Model geometry of microstructure at the velocity of the variable component in the line of sight to κ Vel (different from that of the surrounding medium) with a depth transverse to the line of sight of 10 au and an elongated length along the line of sight of 100 au. The interstellar radiation field striking the microstructure transversely to the line of sight drives the chemistry in the microstructure, its intensity falling off with $A_{V,\mathrm{trans}}$. The contribution to column densities from species within the microstructure is calculated along the line of sight through the structure, over a visual extinction $A_{V,\mathrm{long}}$.

We investigate the chemistry in transient microstructure using a PDR code that self-consistently determines the chemistry and thermal balance on a one-dimensional adaptive spatial grid (Papadopoulos et al. 2002; to be described in detail in a subsequent paper). While the physical structure of the slab is assumed fixed, the chemistry within it will be strongly time- and space-dependent. We have chosen gas phase elemental abundances, relative to n_{H}, as follows:

$$\begin{aligned}
\mathrm{He/H} &= 0.075,\\
\mathrm{C/H} &= 1.79\times10^{-4},\\
\mathrm{N/H} &= 8.52\times10^{-5},\\
\mathrm{O/H} &= 4.45\times10^{-4},\\
\mathrm{Na/H} &= 8.84\times10^{-7},\\
\mathrm{Mg/H} &= 5.12\times10^{-6},\\
\mathrm{Si/H} &= 8.21\times10^{-7},\\
\mathrm{S/H} &= 1.43\times10^{-6},\\
\mathrm{Cl/H} &= 1.1\times10^{-7},\\
\mathrm{Ca/H} &= 5.72\times10^{-10},\\
\mathrm{Fe/H} &= 6.19\times10^{-6}.
\end{aligned}$$

The fraction of hydrogen initially contained in H_2 is unknown; the chemistry will depend strongly on this factor. We note that the structures are dense and, if set up as proposed by Hartquist et al. (2003), would be found in post-shock regions. Hence, it is plausible to assume a significant fraction of H_2 in the slab. We have arbitrarily set $n(\mathrm{H_2})/n_{\mathrm{H}} = 0.4$ and we note that the chemical abundances predicted by the model should be proportional to this parameter. Because we are considering the *additional contribution* to molecular species produced by chemistry in the microstructure, all other molecular abundances are set to zero initially. A total of 128 species are included in the model, connected through a network of over 1500 reactions, including ionization and recombination of atoms. Freeze-out and mantle evaporation processes have been neglected as a result of the short time-scales over which these structures evolve and their low visual extinction.

The filamentary or sheet-like nature of such objects is accounted for by assuming that the line of sight is within the slab and at a transverse depth of 10 au from its surface (see Fig. 1). Column densities are then simply proportional to the length of the line of sight within the slab.

Because the physical conditions within these regions are uncertain, a large range of parameter space is examined to provide a thorough investigation of microstructure chemistry. The effect of varying the slab density and age, as well as the environmental parameters of incident radiation field strength and cosmic ray ionization rate (ζ) are all considered, producing a four-dimensional grid of test parameters.

Observational estimates of microstructure density generally vary between $10^3 \leqslant n_{\mathrm{H}} \leqslant 10^5$ cm^{-3}, with some indications of even higher densities. We have explored the model chemistry for this density range and have made some additional calculations for the higher densities suggested by the formaldehyde observations of Moore & Marscher (1995). Slab ages of 1–1000 yr are considered. Radiation strengths and cosmic ray ionization rates of $\frac{1}{3}$, 1 and 3 times the standard interstellar values (1 Habing and 1.3×10^{-17} s^{-1}, respectively) are also considered.

3 MODEL RESULTS

The purpose of our study is to investigate whether there exists a parameter space of densities, radiation fields, cosmic ray ionization rates and dimensions where molecules can be formed in the variable

Table 1. Column densities (cm^{-2}) for molecular species along the line of sight within a microstructure of transverse depth 10 au and elongation factor 10 along the line of sight. The region is subject to standard interstellar radiation and particle fields of 1 Habing (1.6×10^{-3} erg cm^{-2} s^{-1}) and $\zeta = 1.3 \times 10^{-17}$ s^{-1}. Values in bold indicate potentially detectable abundances (with column densities $> 10^{11}$ cm^{-2}).

Species	Time	Density (cm^{-3})				
	(yr)	10^3	5×10^3	10^4	5×10^4	10^5
CO	1	2.11×10^6	1.22×10^8	3.04×10^{10}	$\mathbf{1.20 \times 10^{11}}$	$\mathbf{2.31 \times 10^{11}}$
CO	5	2.03×10^7	7.89×10^{10}	$\mathbf{1.42 \times 10^{11}}$	$\mathbf{3.35 \times 10^{11}}$	$\mathbf{1.26 \times 10^{12}}$
CO	10	4.72×10^7	8.52×10^{10}	$\mathbf{1.57 \times 10^{11}}$	$\mathbf{6.86 \times 10^{11}}$	$\mathbf{2.56 \times 10^{12}}$
CO	50	4.32×10^8	9.93×10^{10}	$\mathbf{2.87 \times 10^{11}}$	$\mathbf{2.87 \times 10^{12}}$	$\mathbf{1.15 \times 10^{13}}$
CO	100	9.54×10^8	3.31×10^{10}	$\mathbf{2.62 \times 10^{11}}$	$\mathbf{5.00 \times 10^{12}}$	$\mathbf{2.04 \times 10^{13}}$
CH	1	7.51×10^8	1.35×10^{10}	$\mathbf{3.74 \times 10^{11}}$	$\mathbf{6.49 \times 10^{11}}$	$\mathbf{1.14 \times 10^{12}}$
CH	5	1.84×10^9	$\mathbf{2.28 \times 10^{11}}$	$\mathbf{4.46 \times 10^{11}}$	$\mathbf{4.79 \times 10^{11}}$	$\mathbf{1.13 \times 10^{12}}$
CH	10	2.12×10^9	$\mathbf{1.37 \times 10^{11}}$	$\mathbf{3.06 \times 10^{11}}$	$\mathbf{4.52 \times 10^{11}}$	$\mathbf{1.02 \times 10^{12}}$
CH	50	2.84×10^9	2.87×10^{10}	$\mathbf{1.18 \times 10^{11}}$	$\mathbf{3.24 \times 10^{11}}$	$\mathbf{7.35 \times 10^{11}}$
CH	100	2.82×10^9	1.51×10^{10}	5.81×10^{10}	$\mathbf{2.77 \times 10^{11}}$	$\mathbf{6.04 \times 10^{11}}$
C_2	1	2.20×10^5	3.05×10^7	1.71×10^9	1.86×10^{10}	7.97×10^{10}
C_2	5	4.32×10^6	4.89×10^9	1.11×10^{10}	8.77×10^{10}	$\mathbf{4.71 \times 10^{11}}$
C_2	10	1.07×10^7	5.76×10^9	1.49×10^{10}	$\mathbf{1.79 \times 10^{11}}$	$\mathbf{8.78 \times 10^{11}}$
C_2	50	8.52×10^7	7.36×10^9	3.64×10^{10}	$\mathbf{5.50 \times 10^{11}}$	$\mathbf{1.77 \times 10^{12}}$
C_2	100	1.66×10^8	5.07×10^9	4.01×10^{10}	$\mathbf{6.09 \times 10^{11}}$	$\mathbf{1.47 \times 10^{12}}$
OH	1	3.23×10^7	4.92×10^8	$\mathbf{9.81 \times 10^{11}}$	$\mathbf{6.58 \times 10^{11}}$	$\mathbf{2.85 \times 10^{11}}$
OH	5	1.56×10^8	$\mathbf{8.13 \times 10^{11}}$	$\mathbf{1.05 \times 10^{12}}$	$\mathbf{2.96 \times 10^{11}}$	$\mathbf{4.10 \times 10^{11}}$
OH	10	3.01×10^8	$\mathbf{4.97 \times 10^{11}}$	$\mathbf{6.58 \times 10^{11}}$	$\mathbf{2.95 \times 10^{11}}$	$\mathbf{3.28 \times 10^{11}}$
OH	50	1.43×10^9	$\mathbf{1.25 \times 10^{11}}$	$\mathbf{2.66 \times 10^{11}}$	$\mathbf{1.72 \times 10^{11}}$	$\mathbf{2.42 \times 10^{11}}$
OH	100	1.98×10^9	1.51×10^{10}	9.12×10^{10}	$\mathbf{1.44 \times 10^{11}}$	$\mathbf{2.42 \times 10^{11}}$

Table 2. Column densities (cm^{-2}) for neutral and singly ionized calcium along the line of sight within a microstructure of transverse depth 10 au and elongation factor 10 along the line of sight. The region is subject to standard interstellar radiation and particle fields.

Species	Time	Density (cm^{-3})				
	(yr)	10^3	5×10^3	10^4	5×10^4	10^5
Ca I	1	5.62×10^4	1.90×10^6	7.49×10^6	1.80×10^8	6.41×10^8
Ca I	5	2.75×10^5	9.28×10^6	3.63×10^7	8.20×10^8	2.73×10^9
Ca I	10	5.39×10^5	1.81×10^7	6.98×10^7	1.46×10^9	4.43×10^9
Ca I	50	2.36×10^6	7.38×10^7	2.64×10^8	3.19×10^9	6.26×10^9
Ca I	100	4.00×10^6	1.17×10^8	3.82×10^8	3.12×10^9	5.13×10^9
Ca II	1	1.10×10^9	4.30×10^9	1.02×10^{10}	5.50×10^{10}	1.13×10^{11}
Ca II	5	1.10×10^9	4.30×10^9	1.02×10^{10}	5.44×10^{10}	1.11×10^{11}
Ca II	10	1.17×10^9	4.82×10^9	9.39×10^9	5.38×10^{10}	1.01×10^{11}
Ca II	50	1.16×10^9	4.76×10^9	9.20×10^9	5.19×10^{10}	9.95×10^{10}
Ca II	100	1.16×10^9	4.72×10^9	9.08×10^9	5.17×10^{10}	1.01×10^{11}

components and also to determine the time-dependent nature of such structures. In the next two subsections, we make predictions, based on our models, of the physical conditions and time-dependence of the microstructure, respectively.

In all the results reported here, we have assumed an elongation factor of 10; i.e. the path-length along the line of sight through the microstructure is 10× the transverse depth, 10 au.

3.1 Physical characteristics of the microstructure

The results of our chemical model suggest that only a few molecular species are formed in large enough quantities in the proposed scenario to be potentially detectable. They include CH, CH_2, CO, C_2 and OH. In our model, these species are only produced in great enough quantities to be detectable under certain physical conditions (see Tables 1 and 2, and Figs 2 and 3). In Table 1, we list the column densities of CO, CH, C_2 and OH as a function of density and time at a transverse depth of 10 au into the microstructure slab, corresponding to a transverse visual extinction of approximately 10^{-4} to 10^{-2} mag for number densities in the range 10^3 to 10^5 cm^{-3}, making the assumption that the elongation factor along the line of sight (described above) is 10. Column densities larger than 10^{11} cm^{-2} are shown in bold in Table 1, indicating a reasonable lower limit for molecular species that are potentially detectable. Assuming that the microstructure has a transverse spatial dimension of 10 au, a minimum density of 10^4 cm^{-3} is necessary for most species to be detectable. Table 2 lists the column densities for Ca I and Ca II. Because atoms have stronger oscillator strengths than molecules,

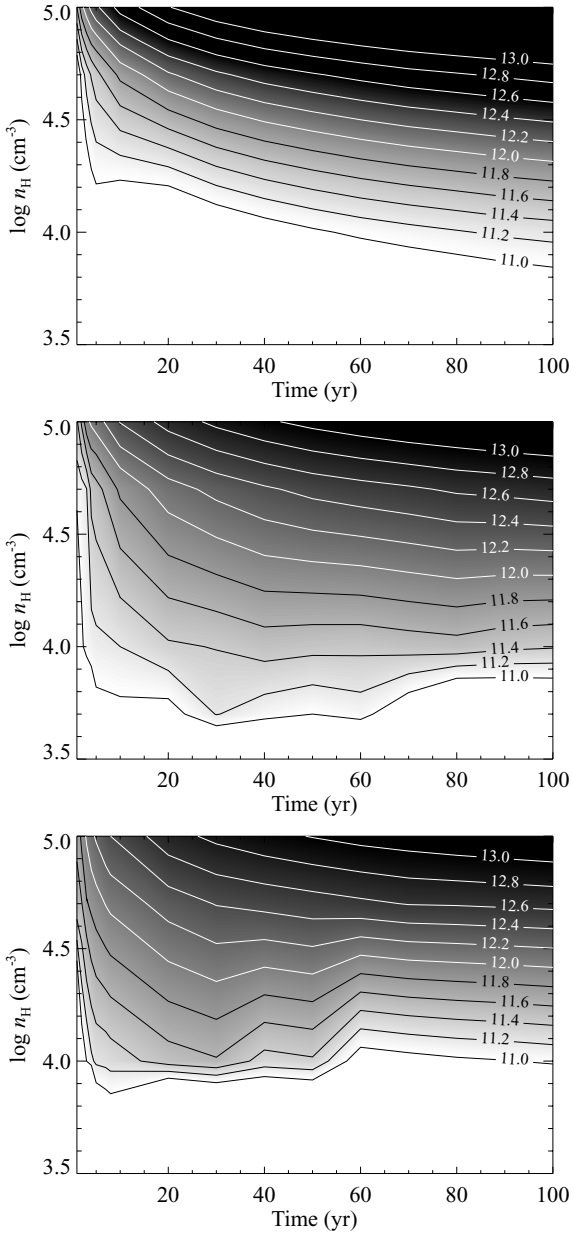

Figure 2. Contours of log CO column density as a function of density and time for a microstructure of transverse depth 10 au, elongated by a factor of 10 along the line of sight, and a cosmic ray ionization rate of $\zeta = 1.3 \times 10^{-17}$ s^{-1}. From top to bottom, the three figures are for incident radiation field strengths of $\frac{1}{3}$, 1 and 3 Habing, respectively.

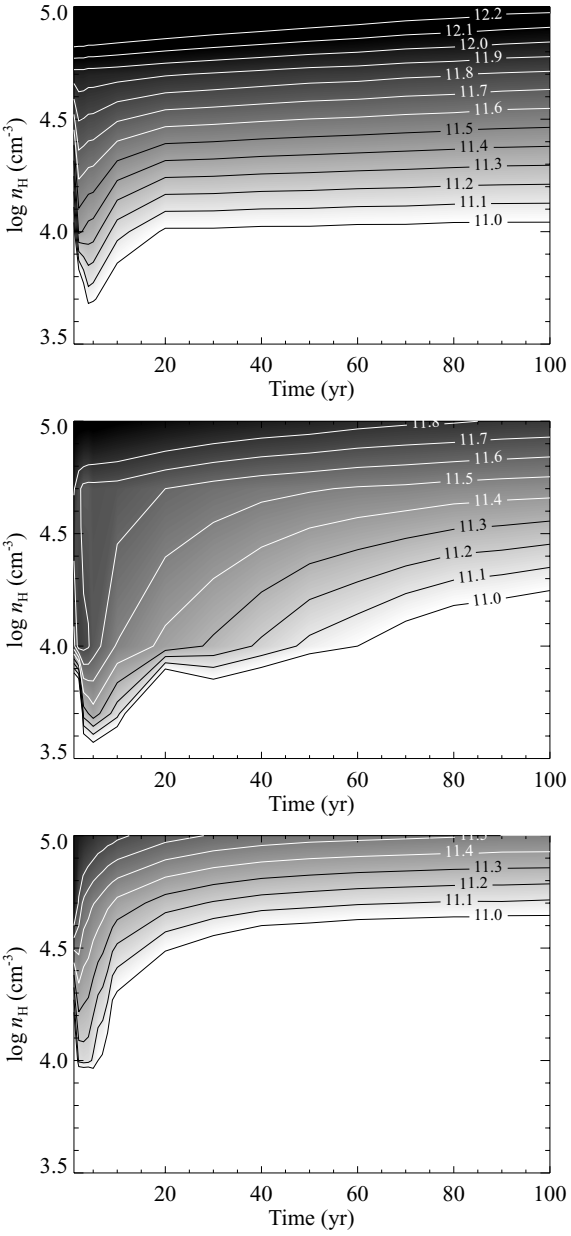

Figure 3. Contours of log CH column density as a function of density and time for a microstructure of transverse depth 10 au, elongated by a factor of 10 along the line of sight, and a cosmic ray ionization rate of $\zeta = 1.3 \times 10^{-17}$ s^{-1}. From top to bottom, the three figures are for incident radiation field strengths of $\frac{1}{3}$, 1 and 3 Habing, respectively.

these species are detectable at lower column densities than the limit of 10^{11} cm^{-2} imposed in Table 1. Figs 2 and 3 show how the column densities of CO and CH behave as a function of density, time and radiation field. We find that CO is particularly sensitive to variations in the number density and its column density can vary by over 2 orders of magnitude in the number density range considered here. Its sensitivity to the radiation field is more subtle: at early times (<20 yr) and low densities ($<10^4$ cm^{-3}), a weak radiation field (<1 Habing) yields a longer time-scale (∼100 yr) for the production of detectable CO. CH, on the other hand, shows a strong sensitivity to the radiation field employed. In fact, if the field is stronger than 1 Habing, CH can only remain detectable at high densities ($>5 \times 10^4$ cm^{-3}). In general, CH is formed and then destroyed very quickly. These trends restrict the parameter space for which both CO and CH can be present in the microstructure *at the same time*. None of the species seem to have a strong dependence on the rate of cosmic ray ionization employed.

The most remarkable result is that, even at the earliest times shown, if the number density is sufficiently high then potentially detectable column densities of the species listed above are attained. Thus, the high density drives a chemistry fast enough to overcome the losses as a result of the strong radiation field. Because the transverse visual extinctions considered are close to zero, the region is essentially unshielded. Note, for example, that the total extinction

along the line of sight towards κ Vel observed by Crawford (2002) is small [$E(B-V)=0.11$] and that the transverse extinction at the variable component must be significantly less than this. By assuming that the transverse extinction is close to zero, we are therefore estimating the lower limit of the additional contribution to column densities from species generated in the microstructure.

The adopted column density of H_2 is, however, sufficiently large to ensure that the H_2 photodissociation rate is too slow to cause significant loss of H_2 on the time-scales considered here.

The fact that high densities are necessary in order to produce sufficiently large molecular abundances in the microstructure is consistent with the conclusions of Moore & Marscher (1995) who find that, if the molecular variability is indeed a result of density structure, the number densities need to be at least 10^6 cm^{-3}. In fact, Marscher et al. (1993) and Moore & Marscher (1995) detect both H_2CO and OH in their time variability study. In our study, OH is present as long as the density is $>5 \times 10^3$ cm^{-3} and does indeed show time variability (see Table 1). H_2CO, however, never reaches a high enough abundance to be detectable for the number densities considered here. In order to see whether densities as high as the ones considered by Moore & Marscher (1995) could produce significant amounts of H_2CO, we ran two more models at 10^6 and 10^7 cm^{-3} under standard interstellar conditions. We find that at 10^6 cm^{-3}, H_2CO is only just barely close to the lower limit of detectability for times $\geqslant 500$ yr, while at 10^7 cm^{-3}, H_2CO becomes detectable after only 50 yr. These models further support the Moore & Marscher (1995) findings.

3.2 Time-dependence of the chemistry

Tables 1 and 2, and Fig. 4 show how the different species behave as a function of time. We now briefly discuss the time variability of each species for number densities $\geqslant 10^4$ cm^{-3}. CO takes ∼5–10 yr to form in significant amounts and its abundance increases steadily with time. For CO to be abundant, therefore, the microstructure would need to exist for at least 10 yr. CH, on the other hand, forms in less than 1 yr, but is subsequently destroyed (in part to form CO) within the first 100 yr. C_2 takes over 10 yr to form in detectable quantities, then survives in the gas for at least 300 yr, although its abundance starts to decline. OH behaves in a similar manner to CH in that it forms within 1 yr but starts being converted into other species almost immediately and by 500 yr its abundance is too low to be detectable. Ca II is present, confirming the detection of Crawford (2002) at the velocity of the microstructure. However, it cannot be used as a diagnostic test of the microstructure age because its abundance is invariant. Ca I, on the other hand, shows considerable time variability, though whether the variations are large enough to be detectable is less certain. Of course, these variations are not reflected in the column densities of Ca II, because its abundance is several orders of magnitude higher. The CO column density under appropriate parameter choices generally exceeds those of other molecular species. Thus, for a number density of 10^4 cm^{-3}, by 100 yr the CO column density has built up to 2.6×10^{11} cm^{-2}, while those for CH and C_2 are 5.8×10^{10} and 4.0×10^{10} cm^{-2}, respectively. Although the amounts by which CH, OH, C_2, etc. decline with time are very small and may therefore seem insignificant, they are indeed real and consistent with the gas phase chemistry that is taking place. The behaviour described above is expected for the usual gas phase chemical networks: CO and C_2 column densities increase monotonically over the time span considered here. A feed molecule for the networks producing CO and C_2 is CH, and its column density declines slightly over this period, showing that CH is being converted into other species; no significant loss of CH by photodissociation occurs in the time interval explored here.

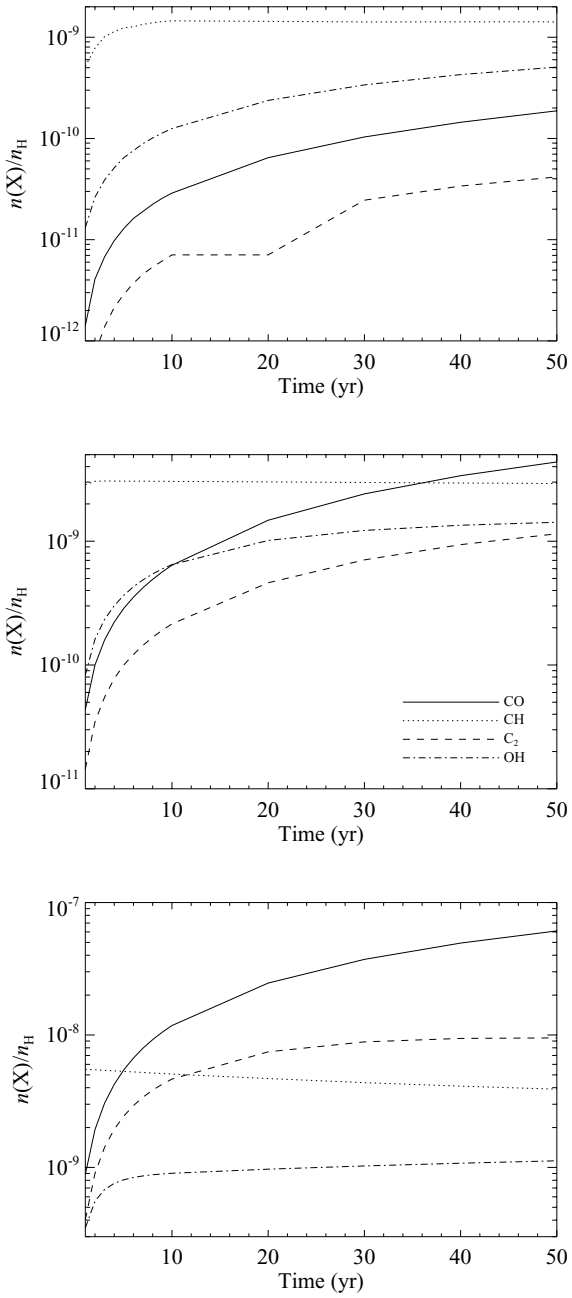

Figure 4. Fractional abundances of CO (solid line), CH (dotted), C_2 (dashed) and OH (dash-dot) at a transverse visual extinction of $A_{V,\mathrm{trans}} = 10^{-4}$ mag into the microstructure, subject to an incident radiation field strength of 1 Habing and a cosmic ray ionization rate of $\zeta = 1.3 \times 10^{-17}$ s^{-1}. From top to bottom, the three figures are for microstructure densities of 10^3, 10^4 and 10^5 cm^{-3}, respectively.

In summary, for CO and C_2 to form, the microstructure needs to survive at least 10 yr. On the other hand, it cannot be much older than ∼50 yr if CH is indeed observed.

Unfortunately, detection of CO by absorption in its resonance line requires a UV spectrometer in an orbital observatory; none is currently available. However, CH and C_2 are detectable from the ground. It appears from this work that these molecules should

have comparable abundances in transient microstructure of number density $\sim 10^4$ cm^{-3}.

4 COMPARISONS WITH OBSERVATIONS AND CONCLUSIONS

This study was prompted in part by the molecular detection obtained by Crawford (2002) at the velocity (different to that of the surrounding medium) of previously reported microstructure in the line of sight towards κ Vel. Hence we now briefly compare our models with such observations. In Table 2 of Crawford (2002), the observed column densities of Ca I, Ca II (two velocity components) and CH are listed, respectively, as 3.2×10^9, 2.0×10^{11} and 6.2×10^{10}, 2.7×10^{11} cm^{-2}. If we assume an elongation factor of 10 along the line of sight and a gas density of the order of $\sim 10^5$ cm^{-3}, the observed CH column density can be easily reached at very early times ($\sim$10 yr) and maintained. If instead the density of the microstructure is closer to 10^4 cm^{-3} then we infer a maximum age for the microstructure of about 50 yr, after which most CH would be destroyed. Hence, observations of CH indicate that such filamentary or sheet-like structures are likely to be younger than 50 yr. The observed Ca I and Ca II column densities can be produced in the model if the microstructure has a number density of $\sim 5 \times 10^4$ cm^{-3} and is older than 10 yr (see Table 2).

In order to further test the predicted molecular abundances, we conducted a high-resolution search for interstellar C_2 at the velocity of the variable component towards κ Vel using the Ultra-High-Resolution Facility (UHRF; Diego et al. 1995) at the Anglo-Australian Telescope in 2003 February. 16 individual exposures were made of the region containing the Q(4) line at 8763.751 Å, with a total integration time of 4.9 h. Data reduction and calibration was as described by Crawford (1997, 2002). The final continuum signal-to-noise ratio was 480, but the Q(4) line was not detected. The resulting 3σ upper limit to the equivalent width of the Q(4) line was 0.09 mÅ, yielding an upper limit to the $J = 4$ column density of $N(J = 4) \leqslant 1.95 \times 10^{11}$ cm^{-2} (using the oscillator strength adopted by Crawford 1997). At the high densities ($n_{\rm H} = 10^3$ to 10^5 cm^{-3}) expected for these variable components, the rotational populations will be approximately thermal and for $T \sim 100$ K we expect the total C_2 column density to be $N(C_2) \sim 4 \times N(J = 4)$ (e.g. van Dishoeck 1984). Thus, our observations imply $N(C_2) \lesssim 10^{12}$ cm^{-2} in the variable interstellar component towards κ Vel. This is consistent with the model results given in Table 1 for $N_{\rm H} \lesssim 10^5$ cm^{-3}. More sensitive searches for C_2 would appear to be worthwhile, as these would be able to constrain the model results at lower densities.

The best matching models for observations at the velocity of the variable component in the κ Vel line of sight seem therefore to be those for a young ($\sim$50 yr), transient ($<$100 yr), high density ($>10^4$ cm^{-3}), small ($\sim$10 au), slightly elongated (by about a factor of 10 along the line of sight) structure, immersed in an ambient radiation field.

The main result of this paper is that essentially unshielded interstellar gas can develop detectable column densities of molecules on very short time-scales ($<$100 yr) for path-lengths of the order of 100 au along the line of sight, if the density is $\sim 10^4$ cm^{-3} or higher. This time and density domain is a region of parameter space not previously explored. The calculations presented here are pseudo-time-dependent, in that the slab structure is fixed.

If the cause of such microstructure is indeed magnetohydrodynamic, then the filamentary objects likely to be responsible for the effects observed towards κ Vel and elsewhere are probably waves moving at magnetosonic sound speed. More complex and realistic models are now being explored (Garrod et al. 2005).

ACKNOWLEDGMENTS

TAB is supported by a Particle Physics and Astronomy Research Council (PPARC) studentship. SV acknowledges individual financial support from a PPARC Advanced Fellowship. DAW thanks the Leverhulme Fund for the Leverhulme Emeritus Award. The authors are very grateful to Dr T. Nguyen for initial studies of these problems. We thank the referee for constructive comments that helped to improve an earlier draft of this paper.

REFERENCES

Blades J. C., Sahu M. S., He L., Crawford I. A., Barlow M. J., Diego F., 1997, ApJ, 478, 648
Cecchi-Pestellini C., Dalgarno A., 2000, MNRAS, 313, L6
Cha A., Sembach K. R., 2000, ApJS, 126, 399
Crawford I. A., 1997, MNRAS, 290, 41
Crawford I. A., 2002, MNRAS, 334, L33
Crawford I. A., Howarth I. D., Ryder S. D., Stathakis R. A., 2000, MNRAS, 319, L1
Danks A. C., Sembach K. R., 1995, AJ, 109, 2627
Danks A. C., Walborn N. R., Vieira G., Landsman W. B., Gales J., Garcia B., 2001, ApJ, 547, L155
Davis R. J., Diamond P. J., Goss W. M., 1996, MNRAS, 283, 1105
Diamond P. J., Goss W. M., Romney J. D., Booth R. S., Kalberla P. M. W., Mebold U., 1989, ApJ, 347, 302
Diego F. et al., 1995, MNRAS, 272, 323
Dieter N. H., Welch W. J., Romney J. D., 1976, ApJ, 206, L113
van Dishoeck E. F., 1984, PhD thesis, Univ. Leiden
Falgarone E., Puget J.-L., Perault M., 1992, A&A, 257, 715
Frail D. A., Weisberg J. M., Cordes J. M., Mathers C., 1994, ApJ, 436, 144
Garrod R. T., Williams D. A., Hartquist T. W., Rawlings J. M. C., Viti S., 2005, MNRAS, 356, 654
Gwinn C. R., 2001, ApJ, 561, 815
Hartquist T. W., Falle S. A. E. G., Williams D. A., 2003, Ap&SS, 288, 369
Hobbs L. M., Ferlet R., Welty D. E., Wallerstein G., 1991, ApJ, 378, 586
Kemp S. N., Bates B., Lyons M. A., 1993, A&A, 278, 542
Langer G. E., Prosser C. F., Sneden C., 1990, AJ, 100, 216
Lauroesch J. T., Meyer D. M., 1999, ApJ, 519, L181
Lauroesch J. T., Meyer D. M., Blades J. C., 2000, ApJ, 543, L43
Liszt H. S., Lucas R., 2000, A&A, 355, 333
Lucas R., Liszt H. S., 1993, A&A, 276, L33
Marscher A. P., Moore E. M., Bania T. M., 1993, ApJ, 419, L101
Meyer D. M., Blades J. C., 1996, ApJ, 464, L179
Moore E. M., Marscher A. P., 1995, ApJ, 452, 671
Papadopoulos P. P., Thi W.-F., Viti S., 2002, ApJ, 579, 270
Pety J., Falgarone E., 2000, A&A, 356, 279
Price R. J., Crawford I. A., Barlow M. J., 2000, MNRAS, 312, L43
Rollinde E., Boissé P., Federman S. R., Pan K., 2003, A&A, 401, 215
Stanimirovic S., Weisberg J. M., Hedden A., Devine K. E., Green J. T., 2003, ApJ, 598, L23
Welty D. E., Fitzpatrick E. L., 2001, ApJ, 551, L175

This paper has been typeset from a TEX/LATEX file prepared by the author.